26. Chen, Y., Groll, M. (2006). Dynamics and shape of bubbles on heating surfaces: A simulation study. International Journal of Heat and Mass Transfer, 49 (5-6), 1115–1128. doi: https://doi.org/10.1016/j.ijheatmasstransfer.2005.07.053
27. Gharib, M., Rambod, E., Shariff, K. (1998). A universal time scale for vortex ring formation. Journal of Fluid Mechanics, 360, 121–140. doi: https://doi.org/10.1017/s0022112097008410
28. Canedo, E. L., Favelukis, M., Tadmor, Z., Talmon, Y. (1993). An experimental study of bubble deformation in viscous liquids in simple shear flow. AIChE Journal, 39 (4), 553–559. doi: https://doi.org/10.1002/aic.690390403
29. Uchiyama, T., Sasaki, S. (2014). Experimental Investigation of the Interaction between Rising Bubbles and Swirling Water Flow. International Journal of Chemical Engineering, 2014, 1–10. doi: https://doi.org/10.1155/2014/358241
30. Yuan, D., Xiao, Z., Chen, D., Zhong, Y., Yan, X., Xu, J., Huang, Y. (2016). Numerical Investigation on Bubble Growth and Sliding Process of Subcooled Flow Boiling in Narrow Rectangular Channel. Science and Technology of Nuclear Installations, 2016, 1–12. doi: https://doi.org/10.1155/2016/7253907


UDC 621.01

DOI: 10.15587/1729-4061.2020.203131

# A ROBOMECH CLASS PARALLEL MANIPULATOR WITH THREE DEGREES OF FREEDOM


**Zh. Baigunchekov**
Director
Scientific and Educational Centre of Digital Technologies and Robotics*
Professor
Department of Mechanical Engineering**

**A. Mustafa**
Doctoral Student
Institute of Industrial Engineering**
E-mail: mustafa_azamat@mail.ru

**T. Sobh**
Professor***

**S. Patel**
Professor***

**M. Utenov**
Professor*

*Al-Farabi Kazakh National University
al-Farabi ave., 71, Almaty, Republic of Kazakhstan, 050040

**Satbayev University
Satpaev str., 22a, Almaty, Republic of Kazakhstan, 050013

***University of Bridgeport
Park ave., 126, Bridgeport, CT 06604, United States of America



***У даній роботі викладені методи структурно-параметричного синтезу і кінематичного аналізу паралельного маніпулятора з трьома ступенями свободи, що працює в циліндричній системі координат. Цей паралельний маніпулятор відноситься до класу RoboMech, оскільки він працює за заданими законами рухів робочого органу і приводів, що спрощує систему управління і покращує її динаміку. Паралельні маніпулятори класу RoboMech працюють з певними структурними схемами і геометричними параметрами їх ланок. Розглянутий паралельний маніпулятор формується шляхом з'єднання вихідної точки з основою з використанням однієї пасивної і двох активних замикаючих кінематичних ланцюгів (ЗКЛ). Пасивний ЗКЛ має нульову ступінь свободи і він не накладає геометричний зв'язок на рух вихідної точки, тому геометричні параметри ланок пасивного ЗКЛ вільно варіюються. Активні ЗКЛ мають активні кінематичні пари і вони накладають геометричні зв'язки на рух вихідної точки. Геометричні параметри ланок активних ЗКЛ визначаються на основі апроксимаційних задач Чебишевського і квадратичного наближень. Для цього складено рівняння геометричних зв'язків у вигляді функцій зважених різниць, які представлені у вигляді узагальнених (Чебишевських) поліномів. Це призводить до лінійних ітераційних задач.***

***Вирішені пряма і зворотна задачі кінематики досліджуваного паралельного маніпулятора. У прямій задачі кінематики за заданими положеннями вхідних ланок визначені координати вихідної точки. У зворотній задачі кінематики за координатами вихідної точки визначаються положення вхідних ланок. Пряма і зворотна задачі кінематики досліджуваного паралельного маніпулятора зводяться до рішень задач про положення діад Сильвестра. Представлені чисельні результати структурно-параметричного синтезу і кінематичного аналізу розглянутого паралельного маніпулятора. Чисельні результати кінематичного аналізу показують, що максимальне відхилення руху вихідної точки від ортогональних траєкторій становить 1,65 %***



***Ключові слова: паралельний маніпулятор, RoboMech, циліндричні системи координат, Чебишевське і квадратичне наближення***

*Received date 25.03.2020*
*Accepted date 11.05.2020*
*Published date 19.06.2020*




## 1. Introduction

Existing methods of designing both serial and parallel manipulating robots are mainly reduced to solving the inverse kinematics problem, i. e. determining the laws of movements of manipulator actuators according to the specified laws of movements of end-effectors, followed by the development of control systems. At the same time, manipulator actuators usually operate in controlled modes of intensive accelerations and decelerations, which worsens their dynamics and reduces efficiency.

Mechanisms, as well as manipulating robots, are designed to move end-effectors according to the specified laws of movements. However, in mechanisms, unlike manipulating robots, the laws of movements of the actuators are set (usually monotonously and evenly). Therefore, setting the laws of movements of the actuators of the designed manipulators, along with the specified laws of movements of the end-effectors, improves their dynamics and increases efficiency. In addition, setting the laws of movements of the actuators significantly simplifies the control system of the designed manipulators.

Parallel manipulators, i. e. manipulators with closed kinematic chains, which possess the property of manipulating robots as the manipulation of moving output objects in accordance with their laws of movements and possess the property of mechanisms as setting the laws of movements of actuators, are called parallel manipulators of a RoboMech class [1–3]. In simultaneously setting the laws of movement of end-effectors and actuators, parallel manipulators of a RoboMech class work under certain structural schemes and geometric parameters of the links.

## 2. Literature review and problem statement

The basis for the structural synthesis of planar mechanisms is proposed in Assur [4, 5], according to which the mechanism is formed by connecting to the input link (actuator) and the base of structural groups with zero degree of freedom (DOF). These structural groups are then called Assur groups. The Assur groups or Assur kinematic chains based composition principle for planar mechanisms is extended for spatial mechanisms [6].

The structure of serial manipulators consists of a manipulator arm, which represents an open kinematic chain with three DOF, and a wrist mechanism with three DOF. The arm of the manipulator delivers the wrist mechanism to the specified position of space, and the wrist mechanism provides the orientation of the gripper.

In a parallel manipulator, the positioning and orientation of the end-effector are performed by a single mechanism, which is a complex closed kinematic chain with numerous types of kinematic pairs. The simplest and most common method of structural synthesis of parallel manipulators is to determine their structural schemes (architecture) by a given number of DOF, links, and kinematic pairs using the Grubler-Kutsbach formula or criterion [7]. This formula establishes a relationship between the number of DOF of the manipulator with the number of links, kinematic pairs, and their mobility, as well as the dimension of the space in which the manipulator operates. In general, the type synthesis of parallel manipulators requires a condition, including the moving characteristics and DOF of terminal components. Before that, it is essential to have a mathematical description of the motion of components. Only in this way, the DOF of the components (or the manipulator) can be acquired correctly. On this issue, several systematic mathematical approaches have been proposed for the type synthesis of parallel manipulators, such as the methods based on the screw theory, on the theory of differential geometry, on the theory of linear transformation, on the displacement group theory, on the single-open-chain units. A review of research on the synthesis of types of parallel robotic mechanisms was made in [8].

In kinematic synthesis (dimensional or parametric synthesis) of mechanisms, with their known structural schemes, the geometric parameters of the links are determined according to the given laws of motions (or discrete positions) of the input and output links. Depending on the type of movements of the output links, kinematic synthesis of mechanisms is divided into the kinematic synthesis of function-generating, path-generating and motion-generating mechanisms. The function-generating mechanism generates a required functional relationship between the displacements of its input and output links. The path-generating mechanism generates a given path of its output point on a floating link. The motion-generating (or rigid body guidance) mechanism generates the given motion of the output link.

Generation of the specified movements of output links can be performed exactly and approximately. Exact reproduction of the required movements of a rigid body by linkage mechanisms is possible with a limited number of positions, depending on the structural scheme of the mechanism-generator, while the possibility of their approximate reproduction is not limited to the number of specified positions.

Exact methods for synthesis of mechanisms or called geometric methods, for the synthesis of mechanisms are based on kinematic geometry. The fundamentals of kinematic geometry for finite positions of a rigid body in a plane motion were developed by Burmester and for finite positions of a rigid body in space were developed by Shoenflies. Burmester in [9] developed the theory of a moving plane having four and five positions on circles. Shoenflies in [10] formulated theorems on the geometrical places of points of a rigid body having seven positions on a circle and three positions on a line. The graphical methods of Burmester and Schoenflies theories received an analytical interpretation, which is summarized in the monograph [11].

Geometric methods of mechanism synthesis are clarity and simple. However, these methods are applicable only for a limited number of positions. Moreover, the algorithms for solving problems using these methods depend significantly on the number of specified positions, and their complexity increases with the number of positions. Approximation (algebraic) methods of mechanism synthesis are devoid of these disadvantages.

Problems of approximation synthesis of mechanisms were first formulated and solved in [12]. Least-square approximations are the most widely used in the approximation synthesis of mechanisms. For the development of this method, a new deviation function-a weighted difference with a parametric weight, proposed in [13], was important. In contrast to the actual deviation, the weighted difference can be reduced to linear forms (generalized polynomials). This makes it quite easy to apply linear approximation methods to the synthesis of mechanisms. This eliminates the limit on the maximum number of specified positions of the moving object.

Combining the main advantages of geometric and approximation methods, a new direction-approximation kinematic geometry of mechanism synthesis was formulated. It studies a special class of approximation problems related to the definition of points and lines of a rigid body describing the constraint of the synthesizing kinematic chains. In the works [14, 15], the basics of approximation kinematic geometry of the plane and spatial movements are presented, where circular square points [14] and points with approximately spherical and coplanar trajectories [15] are defined, which correspond to binary links of the type RR, SS, $SP_k$. Further, in the works [16, 17], the concept of discrete Chebyshev approximations was introduced for the kinematic synthesis of linkage mechanisms. Theorems characterizing the Chebyshev circle and straight line in plane motion [16] and the Chebyshev sphere and plane in spatial motion [17], as well as iterative algorithms for determining Chebyshev circular, spherical and other points based on minimizing the limit values of the weighted difference are formulated.

Similar studies on the kinematic geometry of the plane and spatial motions were given in [18]. In [19–21], six-bar linkages for function motion and path generation by means of polynomial homotopic continuation algorithms were synthesized.

The literature review shows that the structural and kinematic synthesis of the designed manipulator is carried out separately. At the same time, it is possible that the geometric parameters of the synthesizing parallel manipulator links of the considered structure may not provide the required laws of motions of the output object. Therefore, it is advisable to carry out kinematic synthesis in conjunction with the structural synthesis of the designed manipulator.

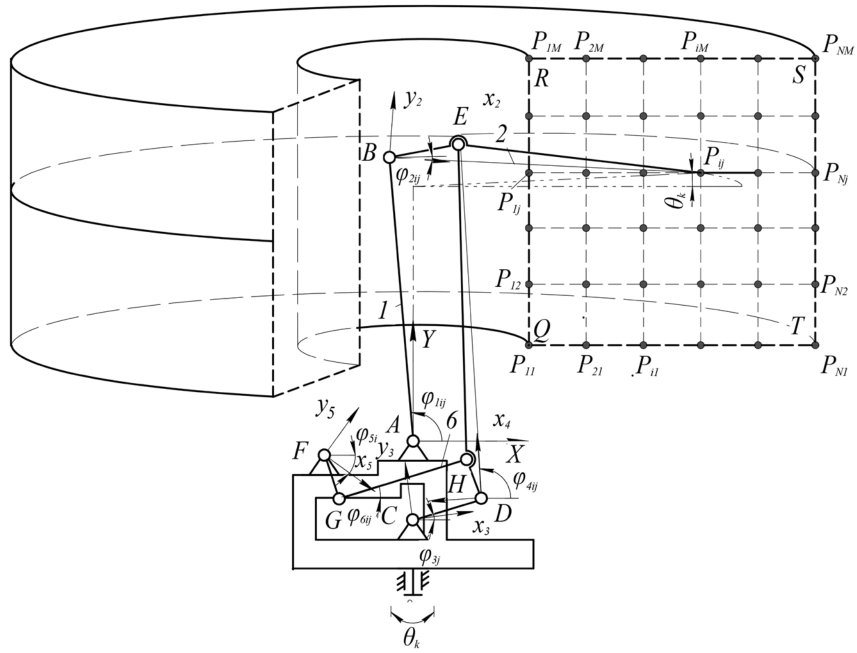


Fig. 1. Parallel manipulator with 3 DOF

According to the developed principle of the formation of mechanisms and manipulators [1], this parallel manipulator is formed by connecting the output object (point *P*) to the base using three closing kinematic chains (CKC): one passive *ABP* and two active *CDE* and *FGH* in the following sequence: firstly, the point *P* is connected to the base using the passive CKC ABP, reaching all the specified positions of the point *P* along the *OX* and *OY* axes, then we connect the active CKC *CDE* whose active kinematic pair *C* reproduces the coordinates $Y_{Pj}$ along the vertical lines, lastly, we connect the next active CKC *FGH*, whose active kinematic pair *F* reproduces the coordinates $X_{Pi}$ along the horizontal lines. The rotation on the angle $\theta_k$ is carried out by rotating the entire manipulator around the axis *OY*.

## 3. The aim and objectives of the study

The aim of the research is the structural-parametric synthesis of a RoboMech class parallel manipulator with three DOF, operating in a cylindrical coordinate system.

To achieve this aim, the following objectives are set:

– to develop the method of structural synthesis;

– to develop the method of parametric synthesis;

– to solve the direct and inverse kinematics problems;

– to carry out a numerical experiment to assess the reliability of the results.

## 4. Structural synthesis

Let be given *N* and *M* values of the coordinates $X_{Pi}$ ($i$==1, 2,..., $N$), and $Y_{Pj}$ ($j$=1, 2,...., M) of the point *P* along the axes *X* and *Y*, respectively, and *K* values of the angle $\theta_k$ ($k$==1, 2,..., $K$) around the axis *Y* in a cylindrical coordinate system (Fig. 1). It is necessary to determine the structural scheme and geometrical parameters of links of a RoboMech class parallel manipulator with three DOF, in which each actuator reproduces these three types of the end-effector movements.

Fig. 2 shows the block structure of the formed parallel manipulator.

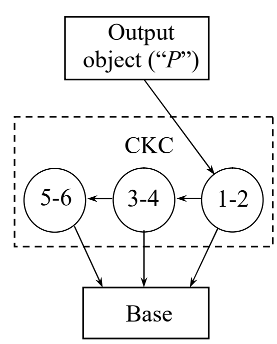


Fig. 2. Block structure of the parallel manipulator with 3 DOF

## 5. Parametric synthesis

According to the block structure of the formed parallel manipulator, its parametric synthesis is carried out on the basis of the parametric synthesis of the CKC in the following sequence: firstly, the passive CKC *ABP*, secondly, the active CKC *CDE*, and thirdly, the active CKC *FGH*. Since the passive CKC *ABP* does not impose geometrical constraints on the movement of the output object (point $P$), its synthesis parameters $\mathbf{p}_1=\left[l_{AB},l_{BP}\right]^{\mathrm{T}}$ are chosen arbitrarily, taking into account the conditions

$$\left|l_{AB}-l_{BP}\right|\le\rho_{\min},\ l_{AB}+l_{BP}\ge\rho_{\max}, \tag{1}$$

where ρ is the variable distance between the points $A$ and $P$, $l_{AB}$ and $l_{BP}$ are the lengths of the links $AB$ and $BP$.

For the parametric synthesis of the active CKC $CDE$, the coordinate system $Cx_3y_3$ is fixed to the active joint $C$, whose $Cx_3$ axis direction shows the angle $\varphi_{3j}$ of rotation of the input link 3. The coordinate system $Bx_2y_2$ is fixed to the point $B$ of the passive CKC $ABP$, whose $Bx_2$ axis directions coincide with the direction of the link $BP$. Coordinates $X_{B_{ij}},Y_{B_{ij}}$ of the origin $B$ and the direction of the axis $Bx_2$ of the coordinate system $Bx_2y_2$ are determined by the equations

$$\begin{bmatrix}X_{B_{ij}}\\ Y_{B_{ij}}\end{bmatrix}=l_{AB}\begin{bmatrix}\cos\varphi_{(AB)_{ij}}\\ \sin\varphi_{(AB)_{ij}}\end{bmatrix}, \tag{2}$$

$$\varphi_{2_{ij}}=\mathrm{tg}^{-1}\left(\frac{Y_{P_{ij}}-Y_{B_{ij}}}{X_{P_{ij}}-X_{B_{ij}}}\right), \tag{3}$$

where

$$\varphi_{(AB)_{ij}}=\mathrm{tg}^{-1}\frac{Y_{P_{ij}}}{X_{P_{ij}}}\pm\cos^{-1}\frac{l_{AP_{ij}}^2+l_{AB}^2-l_{BP}^2}{2l_{AP_{ij}}\cdot l_{AB}}. \tag{4}$$

The signs "+" and "–" in the equation (4) are chosen depending on the assembly of the CKC $ABP$. Then the synthesis parameters of the active CKC $CDE$ are $X_C$, $Y_C$, $x_D^{(3)}$, $y_D^{(3)}$, $x_E^{(2)}$, $y_E^{(2)}$, $l_{DE}$, where $X_C$, $Y_C$, $x_D^{(3)}$, $y_D^{(3)}$, $x_E^{(2)}$, $y_E^{(2)}$ are the coordinates of the joints $C$, $D$, $E$ in the absolute coordinate system $AXY$ and in the local coordinate systems $Cx_3y_3$ and $Bx_2y_2$, respectively, $l_{DE}$ is the length of the link $DE$.

Let denote these synthesis parameters by the vector

$$\mathbf{p}_2=\left[X_C,Y_C,x_D^{(3)},y_D^{(3)},x_E^{(2)},y_E^{(2)},l_{DE}\right]^{\mathrm{T}},$$

and write a $CDEBC$ vector loop-closure equation

$$\bar{R}_C+\Gamma\left(\varphi_{3j}\right)\mathbf{r}_D^{(3)}+\bar{l}_{(DE)_{ij}}=\bar{R}_{B_{ij}}+\Gamma\left(\varphi_{2ij}\right)\mathbf{r}_E^{(2)}, \tag{5}$$

where

$$\bar{R}_C=\left[X_C,Y_C\right]^{\mathrm{T}},\ \mathbf{r}_D^{(3)}=\left[x_D^{(3)},y_D^{(3)}\right]^{\mathrm{T}},\ \bar{R}_{B_{ij}}=\left[X_{B_{ij}},Y_{B_{ij}}\right]^{\mathrm{T}},$$

$$\bar{l}_{(DE)_{ij}}=\left[l_{DE}\cos\varphi_{(DE)_{ij}},l_{DE}\sin\varphi_{(DE)_{ij}}\right]^{\mathrm{T}},\ \mathbf{r}_E^{(2)}=\left[x_E^{(2)},y_E^{(2)}\right]^{\mathrm{T}},$$

$$\Gamma\left(\varphi_{3j}\right)=\begin{bmatrix}\cos\varphi_{3j} & -\sin\varphi_{3j}\\ \sin\varphi_{3j} & \cos\varphi_{3j}\end{bmatrix},$$

$$\Gamma\left(\varphi_{2ij}\right)=\begin{bmatrix}\cos\varphi_{2ij} & -\sin\varphi_{2ij}\\ \sin\varphi_{2ij} & \cos\varphi_{2ij}\end{bmatrix}.$$

Eliminating the unknown angle $\varphi_{(DE)_{ij}}$ from the equation (5) we obtain

$$\left[\bar{R}_C+\Gamma\left(\varphi_{3j}\right)\mathbf{r}_D^{(3)}-\bar{R}_{B_{ij}}-\Gamma\left(\varphi_{2ij}\right)\mathbf{r}_E^{(2)}\right]^2-l_{DE}^2=0. \tag{6}$$

Equation (6) is the equation of the geometrical constraint imposed by the active CKC $CDE$ on the motion of the output point $P$. The problem of determining the geometrical parameters of the links at which such geometrical constraint is approximately realized is the problem of parametric synthesis of the active CKC $CDE$.

The left side of the equation (6) is denoted by $\Delta q_{1ij}$, which is a weighted difference function

$$\Delta q_{1ij}=\left[\bar{R}_C+\Gamma(\varphi_{3j})\mathbf{r}_D^{(3)}-\bar{R}_{B_{ij}}-\Gamma(\varphi_{2ij})\mathbf{r}_E^{(2)}\right]^2-l_{DE}^2. \tag{7}$$

The geometrical interpretation of function (7) is the deviation of the trajectories of the joints $D$ and $E$ from circles with centers in the joints $D$ and $E$ and the radius $l_{DE}$, and the minimization of this function is the connection of the planes $Cx_3y_3$ and $Bx_2y_2$ by the binary link $DE$ of type RR, where R is a revolute joint. After transformation the equation (7) and the next change of variables

$$\begin{bmatrix}p_1\\ p_2\end{bmatrix}=\begin{bmatrix}X_C\\ Y_C\end{bmatrix},\ \begin{bmatrix}p_4\\ p_5\end{bmatrix}=\begin{bmatrix}x_E^{(2)}\\ y_E^{(2)}\end{bmatrix},\ \begin{bmatrix}p_6\\ p_7\end{bmatrix}=\begin{bmatrix}x_D^{(3)}\\ y_D^{(3)}\end{bmatrix},$$

$$p_3=\frac{1}{2}\left(X_C^2+Y_C^2+x_D^{(3)^2}+y_D^{(3)^2}+x_E^{(2)^2}+y_E^{(2)^2}-l_{DE}^2\right), \tag{8}$$

the function $\Delta q_{1ij}$ is represented as the linear forms by groups of synthesis parameters $\mathbf{p}_2^{(k)}$

$$\Delta q_{1ij}^{(k)}=2\left(\mathbf{g}_{ij}^{(k)^{\mathrm{T}}}\mathbf{p}_2^{(k)}-g_{0ij}^{(k)}\right),\ (k=1,2,3), \tag{9}$$

where

$$\mathbf{p}_2^{(1)}=\left[p_1,p_2,p_3\right]^{\mathrm{T}},\ \mathbf{p}_2^{(2)}=\left[p_4,p_5,p_3\right]^{\mathrm{T}},\ \mathbf{p}_2^{(3)}=\left[p_6,p_7,p_3\right]^{\mathrm{T}}, \tag{10}$$

$$\mathbf{g}_{ij}^{(1)}=\begin{bmatrix}-X_{B_{ij}}\\ -Y_{B_{ij}}\\ 1\end{bmatrix}+\left[\begin{array}{cc:c}\multicolumn{2}{c:}{\Gamma\left(\varphi_{2ij}\right)} & 0\\ & & 0\\ \hdashline 0 & 0 & 1\end{array}\right]\cdot\begin{bmatrix}p_4\\ p_5\\ 0\end{bmatrix}+\left[\begin{array}{cc:c}\multicolumn{2}{c:}{\Gamma\left(\varphi_{3j}\right)} & 0\\ & & 0\\ \hdashline 0 & 0 & 1\end{array}\right]\cdot\begin{bmatrix}p_6\\ p_7\\ 0\end{bmatrix}, \tag{11}$$

$$\mathbf{g}_{ij}^{(2)}=\left[\begin{array}{cc:c}\multicolumn{2}{c:}{\Gamma^T\left(\varphi_{2ij}\right)} & 0\\ & & 0\\ \hdashline 0 & 0 & 1\end{array}\right]\cdot\begin{bmatrix}X_{B_{ij}}-p_1\\ Y_{B_{ij}}-p_2\\ 1\end{bmatrix}-\left[\begin{array}{cc:c}\multicolumn{2}{c:}{\Gamma\left(\varphi_{3j}-\varphi_{2ij}\right)} & 0\\ & & 0\\ \hdashline 0 & 0 & 1\end{array}\right]\cdot\begin{bmatrix}p_6\\ p_7\\ 0\end{bmatrix}, \tag{12}$$

$$\mathbf{g}_{ij}^{(3)}=\left[\begin{array}{cc:c}\multicolumn{2}{c:}{\Gamma^T\left(\varphi_{3j}\right)} & 0\\ & & 0\\ \hdashline 0 & 0 & 1\end{array}\right]\cdot\begin{bmatrix}p_1-X_{B_{ij}}\\ p_2-Y_{B_{ij}}\\ 1\end{bmatrix}-\left[\begin{array}{cc:c}\multicolumn{2}{c:}{\Gamma^T\left(\varphi_{3j}-\varphi_{2ij}\right)} & 0\\ & & 0\\ \hdashline 0 & 0 & 1\end{array}\right]\cdot\begin{bmatrix}p_4\\ p_5\\ 0\end{bmatrix}, \tag{13}$$

$$g_{0ij}^{(1)}=-\frac{1}{2}\left[X_{B_{ij}}^2+Y_{B_{ij}}^2\right]-\left[X_{B_{ij}},Y_{B_{ij}}\right]\cdot\Gamma\left(\varphi_{2ij}\right)\cdot\begin{bmatrix}p_4\\ p_5\end{bmatrix}+$$
$$+\left[X_{B_{ij}},Y_{B_{ij}}\right]\cdot\Gamma\left(\varphi_{3j}\right)\cdot\begin{bmatrix}p_6\\ p_7\end{bmatrix}+\left[p_4,p_5\right]\cdot\Gamma\left(\varphi_{3j}-\varphi_{2ij}\right)\cdot\begin{bmatrix}p_6\\ p_7\end{bmatrix}, \tag{14}$$

$$g_{0ij}^{(2)}=-\frac{1}{2}\left[X_{B_{ij}}^2-Y_{B_{ij}}^2\right]-\left[p_1-X_{B_{ij}},p_2-Y_{B_{ij}}\right]\cdot\Gamma\left(\varphi_{3j}\right)\cdot\begin{bmatrix}p_6\\ p_7\end{bmatrix}, \tag{15}$$

$$g_{0ij}^{(3)}=-\frac{1}{2}\left[X_{B_{ij}}^2-Y_{B_{ij}}^2\right]-\left[X_{B_{ij}}-p_1,Y_{B_{ij}}-p_2\right]\cdot\Gamma\left(\varphi_{2ij}\right)\cdot\begin{bmatrix}p_4\\ p_5\end{bmatrix}. \tag{16}$$

The linear representability of function (9) allows to formulate and solve the Chebyshev and least-square approximations for parametric synthesis [11]. In the Chebyshev approximation problem, the vectors of synthesis parameters are determined from the minimum of the functional

$$S^{(k)}\left(\mathbf{p}_2^{(k)}\right)=\max_{\substack{i=\overline{1,N}\\ j=\overline{1,M}}}\left|\Delta q_{ij}^{(k)}\left(\mathbf{p}_2^{(k)}\right)\right|^2\to\min_{p_2^{(k)}} S^{(k)}\left(\mathbf{p}_2^{(k)}\right). \tag{17}$$

In the least-square approximation problem, the synthesis parameter vectors are determined from the minimum of the functional

$$S^{(k)}\left(\mathbf{p}_2^{(k)}\right)=\sum_{i=1}^{N}\sum_{j=1}^{M}\left|\Delta q_{ij}^{(k)}\left(\mathbf{p}_2^{(k)}\right)\right|^2\to\min_{\mathbf{p}_2^{(k)}} S^{(k)}\left(\mathbf{p}_2^{(k)}\right). \tag{18}$$

The linear representability of the equations (7) in the form (9) allows to use the kinematic inversion method, which is an iterative process, at each step of which one group of synthesis parameters $\mathbf{p}_2^{(k)}$ is determined to solve the Chebyshev approximation problem (17). In this case, the linear programming problem is solved. To do this, we introduce a new variable $p'=\varepsilon$, where $\varepsilon$ is the required approximation accuracy. Then the minimax problem (17) is reduced to the following linear programming problem: determine the minimum of the sum

$$\sigma=\mathbf{c}^{\mathrm{T}}\cdot\mathbf{x}\to\min\sigma, \tag{19}$$

with the following constraints

$$\mathbf{h}'^{\mathrm{T}}_{ij}\cdot\mathbf{x}+h_{0ij}\geq 0,\ \mathbf{h}''^{\mathrm{T}}\cdot\mathbf{x}-h_{0ij}\geq 0, \tag{20}$$

where

$$\mathbf{c}=\left[0,...,0.1\right]^{\mathrm{T}},\ \mathbf{x}=\left[\mathbf{p}_2^{(k)},p'\right]^{\mathrm{T}},\ \mathbf{h}'_{ij}=\left[-\mathbf{g}_{ij}^{(k)},0.5\right]^{\mathrm{T}}, \tag{21}$$

$$\mathbf{h}''=\left[\mathbf{g}_{ij}^{(k)},0.5\right]^{\mathrm{T}},\ h_{0ij}=g_{0ij}. \tag{22}$$

The sequence of the obtained values of the function $S^{(k)}$ will decrease and have a limit as a sequence bounded below, because $S^{(k)}(\mathbf{p}_2^{(k)})\geq 0$ for any $\mathbf{p}_2^{(k)}$.

Let consider the least-square approximation problem (18) for the synthesis of active CKC *CDE*. The necessary conditions for the minimum of functions (18) with respect to the parameters $\mathbf{p}_2^{(k)}$

$$\frac{\partial S_{ij}^{(k)}}{\partial\mathbf{p}_2^{(k)}}=0, \tag{23}$$

lead to the systems of linear equations

$$\mathbf{H}^{(k)}\cdot\mathbf{p}_2^{(k)}=\mathbf{h}^{(k)}, \tag{24}$$

where

$$\mathbf{H}^{(k)}=\sum_{i=1}^{N}\sum_{j=1}^{M}\begin{bmatrix} g_{1ij}^{(k)2} & g_{1ij}^{(k)}g_{2ij}^{(k)} & g_{1ij}^{(k)2}\\ g_{1ij}^{(k)}\cdot g_{2ij}^{(k)} & g_{2ij}^{(k)^2} & g_{2ij}^{(k)2}\\ g_{1ij} & g_{2ij}^{(k)2} & 1\end{bmatrix}, \tag{25}$$

$$\mathbf{h}^{(k)}=\sum_{i=1}^{N}\sum_{j=1}^{M}\begin{bmatrix} g_{1ij}^{(k)}\cdot g_{0ij}^{(k)}\\ g_{2ij}^{(k)}\cdot g_{0ij}^{(k)}\\ g_{0ij}\end{bmatrix}. \tag{26}$$

Solving these systems of linear equations for each group of synthesis parameters for given values of the remaining groups of synthesis parameters, we determine their values

$$\mathbf{p}_2^{(k)}=\mathbf{H}^{(k)^{-1}}\cdot\mathbf{h}^{(k)}, \tag{27}$$

at $\det(\mathbf{H}^{(k)})\neq 0$. If $\det(\mathbf{H}^{(k)})=0$, then the revolute kinematic pair is replaced by a prismatic kinematic pair.

It is easy to show that the Hessian of the matrix $\mathbf{H}^{(k)}$ is positively defined together with the main minors. Then the solutions of the systems of linear equations (25) correspond to the minimums of the functions $S^{(k)}$. Thus, the least-square approximation problem (18) can be solved by the linear iteration method, at each step of which one group of synthesis parameters $\mathbf{p}_2^{(k)}$ is determined. The sequence of values of the functions $S^{(k)}$ will be decreasing and have a limit as a sequence bounded.

Let consider the parametric synthesis of the next active CKC *FGH*. To do this, the coordinate system $Fx_5y_5$ is fixed to the active joint *F* whose axis $Fx_5$ shows the angle $\varphi_{5i}$ of rotation of the input link 5, and the coordinate system $Dx_4y_4$ is fixed to the point *D* of the first active CKC *CDE*, whose axis $Dx_4$ is directed along the link *DE*. Then the synthesis parameters of the active CKC *FGH* are $X_F$, $Y_F$, $x_G^{(5)}$, $y_G^{(5)}$, $x_H^{(4)}$, $y_H^{(4)}$, $l_{GH}$, where $X_F$, $Y_F$, $x_G^{(5)}$, $y_G^{(5)}$, $x_H^{(4)}$, $y_H^{(4)}$ are the coordinates of the joints *F,G,H* in the absolute coordinate system *AXY*, in the local coordinate systems $Fx_5y_5$, $Dx_4y_4$, respectively, $l_{GH}$ is the length of the link *GH*. We denote these synthesis parameters by the vector

$$\mathbf{p}_3=\left[X_F,Y_F,x_G^{(5)},y_G^{(5)},x_H^{(4)},y_H^{(4)},l_{GH}\right]^{\mathrm{T}}.$$

Let write an *FG HDE* vector loop-closure equation

$$\overline{R}_F+\Gamma\left(\varphi_{5i}\right)\mathbf{r}_G^{(5)}+\overline{l}_{(GH)_{ij}}=\overline{R}_{D_j}+\Gamma\left(\varphi_{4i}\right)\mathbf{r}_H^{(4)}, \tag{28}$$

where

$$\overline{R}_F=\left[X_F,Y_F\right]^{\mathrm{T}},\ \mathbf{r}_G^{(5)}=\left[x_G^{(5)},y_G^{(5)}\right]^{\mathrm{T}},\ \overline{R}_{D_j}=\left[X_{D_j},Y_{D_j}\right]^{\mathrm{T}},$$

$$\overline{l}_{(GH)_{ij}}=\left[l_{GH}\cos\varphi_{(GH)_{ij}},l_{GH}\sin\varphi_{(GH)_{ij}}\right]^{\mathrm{T}},$$

$$\mathbf{r}_H^{(4)}=\left[x_H^{(4)},y_H^{(4)}\right]^{\mathrm{T}},$$

$$\Gamma\left(\varphi_{5i}\right)=\begin{bmatrix}\cos\varphi_{5i} & -\sin\varphi_{5i}\\ \sin\varphi_{5i} & \cos\varphi_{5i}\end{bmatrix},$$

$$\Gamma\left(\varphi_{4ij}\right)=\begin{bmatrix}\cos\varphi_{4ij} & -\sin\varphi_{4ij}\\ \sin\varphi_{4ij} & \cos\varphi_{4ij}\end{bmatrix}.$$

Eliminating the unknown angle $\varphi_{(GH)_{ij}}$ from the equation (28) yields

$$\left[(\overline{R}_F+\Gamma\left(\varphi_{5i}\right)\mathbf{r}_G^{(5)}-\overline{R}_{D_{ij}}-\Gamma\left(\varphi_{4ij}\right)\mathbf{r}_H^{(4)}\right]^2-l_{GH}^2=0. \tag{29}$$

Equation (29) is the equation of the geometrical constraint imposed by the active CKC *FGH* on the motion of the output point *P*. The problem of determining the geometrical parameters of the links at which such geometrical constraint is approximately realized is the problem of the parametric synthesis of the active CKC *FGH*.

The left side of the equation (29) is denoted by $\Delta q_{2ij}$, which is a function of the weighted difference

$$\Delta q_{2ij} = \begin{bmatrix} \bar{R}_F + \Gamma(\varphi_{5i})\mathbf{r}_G^{(5)} - \bar{R}_C - \\ -\Gamma(\varphi_{3j})\mathbf{r}_D^{(3)} - \Gamma(\varphi_{4ij})\mathbf{r}_H^{(4)} \end{bmatrix}^2 - l_{GH}^2. \quad (30)$$

The geometrical interpretation of function (30) is the deviation of the trajectories of the joints $G$ and $H$ from circles with centers in the joints $G$ and $H$ and the radius $l_{GH}$, and the minimization of this function is the connection of the planes $Fx_5y_5$ and $Dx_4y_4$ by the binary link $GH$ of type RR.

After transformation the equation (30) and the next change of variables

$$\begin{bmatrix} p_1 \\ p_2 \end{bmatrix} = \begin{bmatrix} X_F \\ Y_F \end{bmatrix}, \begin{bmatrix} p_4 \\ p_5 \end{bmatrix} = \begin{bmatrix} x_H^{(4)} \\ y_H^{(4)} \end{bmatrix}, \begin{bmatrix} p_6 \\ p_7 \end{bmatrix} = \begin{bmatrix} x_G^{(5)} \\ y_G^{(5)} \end{bmatrix},$$

$$p_3 = \frac{1}{2}\left(X_F^2 + Y_F^2 + x_G^{(3)^2} + y_G^{(3)^2} + x_H^{(2)^2} + y_H^{(2)^2} - l_{GH}^2\right), \quad (31)$$

the function $\Delta q_{2ij}$ is represented as the linear forms by groups of synthesis parameters $\mathbf{p}_3^{(k)}$

$$\Delta q_{2ij}^{(k)} = 2\left(\mathbf{g}_{ij}^{(k)^T}\mathbf{p}_3^{(k)} - g_{0ij}^{(k)}\right),\ (k = 1,2,3), \quad (32)$$

where

$$\mathbf{p}_3^{(k)} = [p_1, p_2, p_3]^{\mathrm{T}},\ \mathbf{p}^{(2)} = [p_4, p_5, p_3]^{\mathrm{T}},\ \mathbf{p}^{(3)} = [p_6, p_7, p_3]^{\mathrm{T}}. \quad (33)$$

$$\mathbf{g}_{ij}^{(1)} = -\begin{bmatrix} -X_{D_j} \\ -Y_{D_j} \\ 1 \end{bmatrix} - \left[\begin{array}{cc|c} \multicolumn{2}{c|}{\Gamma(\varphi_{4ij})} & 0 \\ & & 0 \\ \hline 0 & 0 & 1 \end{array}\right] \cdot \begin{bmatrix} p_4 \\ p_5 \\ 0 \end{bmatrix} + \left[\begin{array}{cc|c} \multicolumn{2}{c|}{\Gamma^{-1}(\varphi_{5i})} & 0 \\ & & 0 \\ \hline 0 & 0 & 1 \end{array}\right] \cdot \begin{bmatrix} p_6 \\ p_7 \\ 0 \end{bmatrix}, \quad (34)$$

$$\mathbf{g}_{ij}^{(2)} = \left[\begin{array}{cc|c} \multicolumn{2}{c|}{\Gamma^T(\varphi_{4ij})} & 0 \\ & & 0 \\ \hline 0 & 0 & 1 \end{array}\right] \cdot \begin{bmatrix} X_{D_j} - p_1 \\ Y_{D_j} - p_2 \\ 1 \end{bmatrix} - \left[\begin{array}{cc|c} \multicolumn{2}{c|}{\Gamma(\varphi_{5i} - \varphi_{4ij})} & 0 \\ & & 0 \\ \hline 0 & 0 & 1 \end{array}\right] \cdot \begin{bmatrix} p_6 \\ p_7 \\ 0 \end{bmatrix}, \quad (35)$$

$$\mathbf{g}_{ij}^{(3)} = \left[\begin{array}{cc|c} \multicolumn{2}{c|}{\Gamma^T(\varphi_{5i})} & 0 \\ & & 0 \\ \hline 0 & 0 & 1 \end{array}\right] \cdot \begin{bmatrix} p_1 - X_{D_i} \\ p_2 - Y_{D_i} \\ 1 \end{bmatrix} - \left[\begin{array}{cc|c} \multicolumn{2}{c|}{\Gamma^T(\varphi_{5i} - \varphi_{4ij})} & 0 \\ & & 0 \\ \hline 0 & 0 & 1 \end{array}\right] \cdot \begin{bmatrix} p_4 \\ p_5 \\ 0 \end{bmatrix}. \quad (36)$$

Further, the parametric synthesis of the active CKC *FGH* is carried out similarly to the parametric synthesis of the considered active CKC *CDE* by the Chebyshev and least-square approximations.

## 6. Direct kinematics

In direct kinematics, values of the angles $\varphi_{3j}$ and $\varphi_{5i}$ of the manipulator input links 3 and 5 are given, it is necessary to determine the coordinates $X_{P_{ij}}$ and $Y_{P_{ij}}$ of the output point *P*. In this case, the structural formula of the manipulator has the form

$$\begin{array}{l} \mathrm{I}(5) \rightarrow \mathrm{II}(6,4) \leftarrow \mathrm{I}(3) \\ \qquad\quad \downarrow \\ \qquad \mathrm{II}(1,2). \end{array} \quad (37)$$

Consequently, in the direct kinematics, the position analysis of the group II (6,4) is first solved, then of the group II (1,2). To solve the position analysis of the group II (6,4), we derive a *GHD* vector loop-closure equation

$$l_{GH}\mathbf{e}_{6_{ij}} - l_{DH}\mathbf{e}_{(DH)_{ij}} - l_{(GD)_{ij}}\mathbf{e}_{(GD)_{ij}} = 0, \quad (38)$$

where $l$ denotes the modules of vectors, and $\mathbf{e}$ denotes their unit vectors. In the equation (38), the module and direction of the vector $\overline{GD}_{ij}$ as well as the module of the vector $\overline{DH}_{ij}$ are determined by the expressions

$$l_{(GD)_{ij}} = \left[\left(X_{D_j} - X_{G_i}\right)^2 + \left(Y_{D_j} - Y_{G_i}\right)^2\right]^{\frac{1}{2}}, \quad (39)$$

$$\varphi_{(GD)_{ij}} = \mathrm{tg}^{-1}\frac{Y_{D_j} - Y_{G_i}}{X_{D_j} - X_{G_i}}, \quad (40)$$

$$l_{DH} = \left(x_H^{(4)^2} + y_H^{(4)^2}\right)^{\frac{1}{2}}. \quad (41)$$

Coordinates of the joints $G$ and $D$ in the equations (39) and (40) are determined by the expressions

$$\begin{bmatrix} X_{G_i} \\ Y_{G_i} \end{bmatrix} = \begin{bmatrix} X_F \\ Y_F \end{bmatrix} + \begin{bmatrix} \cos\varphi_{5i} & -\sin\varphi_{5i} \\ \sin\varphi_{5i} & \cos\varphi_{5i} \end{bmatrix} \cdot \begin{bmatrix} x_G^{(5)} \\ y_G^{(5)} \end{bmatrix}, \quad (42)$$

$$\begin{bmatrix} X_{D_j} \\ Y_{D_j} \end{bmatrix} = \begin{bmatrix} X_C \\ Y_C \end{bmatrix} + \begin{bmatrix} \cos\varphi_{3j} & -\sin\varphi_{3j} \\ \sin\varphi_{3j} & \cos\varphi_{3j} \end{bmatrix} \cdot \begin{bmatrix} x_D^{(3)} \\ y_D^{(3)} \end{bmatrix}. \quad (43)$$

To determine the unknown direction of the vector $(\overline{GH})_{ij}$, we transfer the vector $l_{DH}\mathbf{e}_{(DH)_{ij}}$ to the right side of the equation (38) and square its both sides

$$l_{GH}^2 + l_{(GD)_{ij}}^2 - 2l_{GH}l_{(GD)_{ij}}\cos\left(\varphi_{(GD)_{ij}} - \varphi_{6_{ij}}\right) = l_{DH}^2, \quad (44)$$

and obtain

$$\varphi_{6_{ij}} = \varphi_{(GD)_{ij}} + \cos^{-1}\frac{l_{GH}^2 + l_{(GD)_{ij}}^2 - l_{DH}^2}{2l_{GH}l_{(GD)_{ij}}}. \quad (45)$$

Direction of the vector $(\overline{DH})_{ij}$ is determined by the equation

$$\varphi_{(DH)_{ij}} = \mathrm{tg}^{-1}\frac{Y_{H_{ij}} - Y_{D_j}}{X_{H_{ij}} - X_{D_j}}, \quad (46)$$

where

$$\begin{bmatrix} X_{H_{ij}} \\ Y_{H_{ij}} \end{bmatrix} = \begin{bmatrix} X_{G_i} \\ Y_{G_i} \end{bmatrix} + l_{GH}\begin{bmatrix} \cos\varphi_{6ij} \\ \sin\varphi_{6ij} \end{bmatrix}. \quad (47)$$

Let consider the position analysis of the group II (1,2). To do this, we derive an *ABE* vector loop-closure equation

$$l_{AB}\mathbf{e}_{1_{ij}} + l_{BE}\mathbf{e}_{(BE)_{ij}} - l_{(AE)_{ij}}\mathbf{e}_{(AE)_{ij}} = 0, \quad (48)$$

where the module and direction of the vector $(\overline{AE})_{ij}$ are determined by the expressions

$$l_{(AE)_{ij}} = \left(X_{E_{ij}}^2 + Y_{E_{ij}}^2\right)^{\frac{1}{2}}, \quad (49)$$

$$\varphi_{(AE)_{ij}} = \mathrm{tg}^{-1}\frac{Y_{E_{ij}}}{X_{E_{ij}}}. \quad (50)$$

Coordinates of the joint $E$ in the equations (49) and (50) are determined by the expressions

$$\begin{bmatrix} X_{E_{ij}} \\ Y_{E_{ij}} \end{bmatrix} = \begin{bmatrix} X_{D_j} \\ Y_{D_j} \end{bmatrix} + l_{DE} \begin{bmatrix} \cos\varphi_{4ij} \\ \sin\varphi_{4ij} \end{bmatrix}, \quad (51)$$

where

$$\varphi_{4_{ij}} = \varphi_{(DH)_{ij}} - \mathrm{tg}^{-1}\frac{x_H^{(4)}}{y_H^{(4)}}. \quad (52)$$

To determine the unknown direction of the vector $(\overline{AB})_{ij}$, we transfer the vector $l_{BE}\mathbf{e}_{ij}$ to the right side of the equation (48) and square its both sides

$$l_{AB}^2 + l_{(AE)_{ij}}^2 - 2l_{AB}l_{(AE)_{ij}}\cos\left(\varphi_{1_{ij}} - \varphi_{(AE)_{ij}}\right) = l_{BE}^2 \quad (53)$$

and obtain

$$\varphi_{1_{ij}} = \varphi_{(AE)_{ij}} + \cos^{-1}\frac{l_{AB}^2 + l_{(AE)_{ij}}^2 - l_{BE}^2}{2l_{AB}l_{(AE)_{ij}}}. \quad (54)$$

Direction of the vector $(\overline{BE})_{ij}$ is determined by the equation

$$\varphi_{(BE)_{ij}} = \mathrm{tg}^{-1}\frac{Y_{E_{ij}} - Y_{B_{ij}}}{X_{E_{ij}} - X_{B_{ij}}}, \quad (55)$$

where

$$\begin{bmatrix} X_{B_{ij}} \\ Y_{B_{ij}} \end{bmatrix} = l_{AB} \begin{bmatrix} \cos\varphi_{1ij} \\ \sin\varphi_{1ij} \end{bmatrix}. \quad (56)$$

Then the coordinates of the output point $P$ are determined by the equation

$$\begin{bmatrix} X_{P_{ij}} \\ Y_{P_{ij}} \end{bmatrix} = \begin{bmatrix} X_{B_{ij}} \\ Y_{B_{ij}} \end{bmatrix} + l_{BP} \begin{bmatrix} \cos\varphi_{(BP)_{ij}} \\ \sin\varphi_{(BP)_{ij}} \end{bmatrix}, \quad (57)$$

where

$$\varphi_{(BP)_{ij}} = \varphi_{(BE)_{ij}} - \mathrm{tg}\frac{y_E^{(2)}}{x_E^{(2)}}. \quad (58)$$

In the equation (58) $x_E^{(2)}$ and $y_E^{(2)}$ are the coordinates of the joint $E$ in the local coordinate systems $Bx_2y_2$.

## 7. Inverse kinematics

In inverse kinematics, values of the angles $\varphi_{3_j}$ and $\varphi_{5_i}$ of the input links $CD$ and $FG$ are determined on the given coordinates $X_{P_{ij}}$, $Y_{P_{ij}}$ of the manipulator's output point $P$. In this case, the structural formula of the manipulator has the form

$$\mathrm{II}(1,2) \rightarrow \mathrm{II}(3,4) \rightarrow \mathrm{II}(5,6). \quad (59)$$

Therefore, in the inverse kinematics, the position analysis of the group II (1,2), II (3,4), and II (5,6) are successively solved. To solve the position analysis of the group II (1,2), we derive an $ABP$ vector loop–closure equation

$$l_{AB}\mathbf{e}_{1_{ij}} + l_{BP}\mathbf{e}_{2_{ij}} - l_{(AP)_{ij}}\mathbf{e}_{(AP)_{ij}} = 0, \quad (60)$$

where the module and direction of the vector $(\overline{AP})_{ij}$ are determined by the expressions

$$l_{(AP)_{ij}} = \left(X_{P_{ij}}^2 + Y_{P_{ij}}^2\right)^{\frac{1}{2}}, \quad (61)$$

$$\varphi_{(AP)_{ij}} = \mathrm{tg}^{-1}\frac{Y_{P_{ij}}}{X_{P_{ij}}}. \quad (62)$$

To determine the unknown direction of the vector $(\overline{AB})_{ij}$, we transfer the vector $l_{BP}\mathbf{e}_{2_{ij}}$ to the right side of the equation (60) and square its both sides

$$l_{AB}^2 + l_{(AP)_{ij}}^2 - 2l_{AB}l_{(AP)_{ij}}\cos\left(\varphi_{1_{ij}} - \varphi_{(AP)_{ij}}\right) = l_{BP}^2 \quad (63)$$

and obtain

$$\varphi_{1_{ij}} = \varphi_{(AP)_{ij}} + \cos^{-1}\frac{l_{AB}^2 + l_{(AP)_{ij}}^2 - l_{BP}^2}{2l_{AB}l_{(AP)_{ij}}}. \quad (64)$$

Direction of the vector $(\overline{BP})_{ij}$ is determined by the equation

$$\varphi_{2_{ij}} = \mathrm{tg}\frac{Y_{P_{ij}} - Y_{B_{ij}}}{X_{P_{ij}} - X_{B_{ij}}}, \quad (65)$$

where

$$\begin{bmatrix} X_{B_{ij}} \\ Y_{B_{ij}} \end{bmatrix} = l_{AB} \begin{bmatrix} \cos\varphi_{1ij} \\ \sin\varphi_{1ij} \end{bmatrix}. \quad (66)$$

To solve the position analysis of the group II (3,4), we derive a $CDE$ vector loop-closure equation

$$l_{CD}\mathbf{e}_{3j} + l_{DE}\mathbf{e}_{4_{ij}} - l_{(CE)_{ij}}\mathbf{e}_{(CE)_{ij}} = 0, \quad (67)$$

where the module and direction of the vector $(\overline{CE})_{ij}$ are determined by the expressions

$$l_{(CE)_{ij}} = \left[\left(X_{E_{ij}} - X_C\right)^2 + \left(Y_{E_{ij}} - Y_C\right)^2\right]^{\frac{1}{2}}, \quad (68)$$

$$\varphi_{(CE)_{ij}} = \mathrm{tg}^{-1}\frac{Y_{E_{ij}} - Y_C}{X_{E_{ij}} - X_C}. \quad (69)$$

Coordinates of the joint $E$ in the absolute coordinate system $AXY$ in the equations (68) and (69) are determined by the expressions

$$\begin{bmatrix} X_{E_{ij}} \\ Y_{E_{ij}} \end{bmatrix} = \begin{bmatrix} X_{B_{ij}} \\ Y_{B_{ij}} \end{bmatrix} + \begin{bmatrix} \cos\varphi_{2ij} & -\sin\varphi_{2ij} \\ \sin\varphi_{2ij} & \cos\varphi_{2ij} \end{bmatrix} \cdot \begin{bmatrix} x_E^{(2)} \\ y_E^{(2)} \end{bmatrix}. \quad (70)$$

To determine the unknown direction of the vector $(\overline{CD})_i$ in the equation (67), we transfer the vector $l_{DE}\mathbf{e}_{4ij}$ to the right side of the equation and square its both sides

$$l_{CD}^2 + l_{(CE)_{ij}}^2 - 2l_{CD}l_{(CE)_{ij}}\cos\left(\varphi_{(CD)_j} - \varphi_{(CE)_{ij}}\right) = l_{DE}^2 \quad (71)$$

and obtain

$$\varphi_{(CD)_j} = \varphi_{(CE)_{ij}} - \cos^{-1}\frac{l_{CD}^2 + l_{(CE)_{ij}}^2 - l_{DE}^2}{2l_{CD}l_{(CE)_{ij}}}. \quad (72)$$

Then the angle $\varphi_{3_j}$ of the input link 3 is determined by the equation

$$\varphi_{3_j} = \varphi_{(CD)_j} + \mathrm{tg}\frac{y_D^{(3)}}{x_D^{(3)}}. \quad (73)$$

Direction of the vector $(\overline{DE})_{ij}$ is determined by the equation

$$\varphi_{4_{ij}} = \mathrm{tg}\frac{Y_{E_{ij}} - Y_{D_j}}{X_{E_{ij}} - X_{D_j}}, \tag{74}$$

where

$$\begin{bmatrix} X_{D_j} \\ Y_{D_j} \end{bmatrix} = \begin{bmatrix} X_C \\ Y_C \end{bmatrix} + l_{CD}\begin{bmatrix} \cos\varphi_{3_j} \\ \sin\varphi_{3_j} \end{bmatrix}. \tag{75}$$

To solve the position analysis of the group II (5,6), we derive an $FGH$ vector loop–closure equation

$$l_{FG}\mathbf{e}_{(FG)_i} + l_{(GH)_{ij}}\mathbf{e}_{6_{ij}} - l_{(FH)_{ij}}\mathbf{e}_{(FH)_{ij}} = 0, \tag{76}$$

where the module and direction of the vector $(\overline{FH})_{ij}$ are determined by the expressions

$$l_{(FH)_{ij}} = \left[\left(X_{H_{ij}} - X_F\right)^2 + \left(Y_{H_{ij}} - Y_F\right)^2\right]^{\frac{1}{2}}, \tag{77}$$

$$\varphi_{(FH)_{ij}} = \mathrm{tg}^{-1}\frac{Y_{H_{ij}} - Y_F}{X_{H_{ij}} - X_F}. \tag{78}$$

Coordinates of the joint $H$ in the absolute coordinate system $AXY$ in the equations (77) and (78) are determined by the expressions

$$\begin{bmatrix} X_{H_{ij}} \\ Y_{H_{ij}} \end{bmatrix} = \begin{bmatrix} X_{D_j} \\ Y_{D_j} \end{bmatrix} + \begin{bmatrix} \cos\varphi_{4ij} & -\sin\varphi_{4ij} \\ \sin\varphi_{4ij} & \cos\varphi_{4ij} \end{bmatrix} \cdot \begin{bmatrix} x_H^{(4)} \\ y_H^{(4)} \end{bmatrix}. \tag{79}$$

To determine the unknown direction of the vector $(\overline{FG})_i$ in the equation (76), we transfer the vector $l_{(GH)_{ij}}\mathbf{e}_{6ij}$ to the right side of the equation and square its both sides

$$l_{FG}^2 + l_{(FH)_{ij}}^2 - 2l_{FG}l_{(FH)_{ij}}\cos\left(\varphi_{(FG)_i} - \varphi_{(FH)_{ij}}\right) = l_{GH}^2, \tag{80}$$

and obtain

$$\varphi_{(FG)_i} = \varphi_{(FH)_{ij}} - \cos^{-1}\frac{l_{FG}^2 + l_{(FH)_{ij}}^2 - l_{GH}^2}{2l_{FG}l_{(FH)_{ij}}}. \tag{81}$$

Then the angle $\varphi_{5_i}$ of the input link 5 is determined by the equation

$$\varphi_{5_i} = \varphi_{(FG)_i} + \mathrm{tg}^{-1}\frac{y_G^{(5)}}{x_G^{(5)}}. \tag{82}$$

In the equation (82) $x_G^{(5)}$ and $y_G^{(5)}$ are the coordinates of the joint $G$ in the local coordinate systems $Fx_5y_5$.

## 8. Numerical results

On the base of the developed methods, the parallel manipulator of a RoboMech class is synthesized, the output point $P$ of which reproduces the series of vertical and horizontal lines in a rectangular $QRST$, lying on the plane of the absolute coordinate system $AXY$ (Fig. 1). The coordinates of the points $Q$, $T$ and the height $QR$ of this rectangle $QRST$, as well as the numbers $M$ and $N$ of the vertical and horizontal lines, have the following values:

$X_Q = 43.00,\ Y_Q = 33.00,\ X_T = 137.00,$

$Y_T = 33.00,\ QR = 99.00,$

$M = 11,\ N = 11.$

The obtained values of the parametric synthesis:

$l_{AB} = 98.67,\ l_{BP} = 108.69,\ X_C = -0.18,$

$Y_C = -27.54,\ x_D^{(3)} = 24.6,$

$y_D^{(3)} = 3.62,\ x_E^{(2)} = 23.64,$

$y_E^{(2)} = 5.85,\ l_{DE} = 123.75,\ X_F = -31.03,$

$Y_F = -4.9,\ x_G^{(5)} = 13.54,$

$y_G^{(5)} = -9.84,\ x_H^{(4)} = 13.85,$

$y_H^{(4)} = 4.31,\ l_{GH} = 46.56.$

Fig. 3 shows two views of the synthesized parallel manipulator's 3D CAD model.

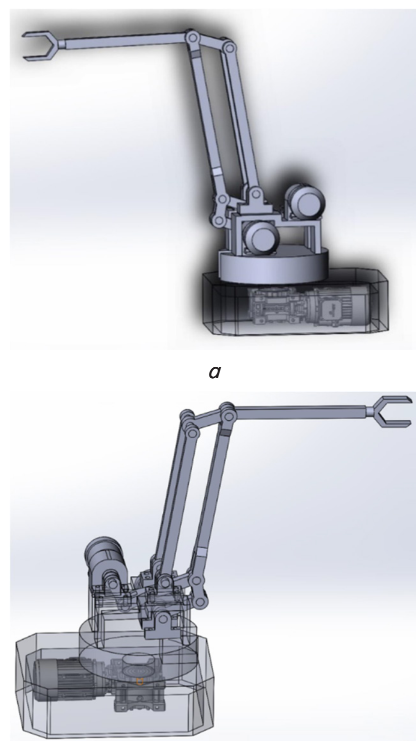

*a*

*b*

Fig. 3. 3D CAD model of the parallel manipulator: *a* – view of the left; *b* – view of the right

The obtained values of the coordinates $X_{P_{ij}}$, $Y_{P_{ij}}$ of the output point $P$ in the given values of the input angles $\varphi_{3j}$ and $\varphi_{5i}$ (direct kinematics) are shown in Table 1. Table 2 shows the obtained values of the output angles $\varphi_{5i}$, $\varphi_{3j}$ in the given values of the input point's $P$ coordinates $X_{P_{ij}}$, $Y_{P_{ij}}$ (inverse kinematics).

An analysis of the results shows that the maximum deviation of the point $P$ motion from the orthogonal trajectories is 1.65 %.

Table 1

The input angles $\varphi_{5i},\varphi_{3i}$ and output point's $P$ coordinates

| $I$ | $j$ | $\varphi_{5i}$ | $\varphi_{3_j}$ | $X_{P_{ij}}$ | $Y_{P_{ij}}$ |
|---|---|---|---|---|---|
| 1 | 2 | 3 | 4 | 5 | 6 |
| 1 | 1 | –95° | –16° | 43.39 | 33.04 |
| 1 | 2 | –95° | –10°30′ | 44.02 | 43.01 |
| 1 | 3 | –95° | –5° | 44.14 | 53.13 |
| 1 | 4 | –95° | 0 | 44 | 62.33 |
| 1 | 5 | –95° | 5° | 43.77 | 71.51 |
| 1 | 6 | –95° | 10°30′ | 43.53 | 81.63 |
| 1 | 7 | –95° | 16° | 43.35 | 91.78 |
| 1 | 8 | –95° | 21°30′ | 43.24 | 101.99 |
| 1 | 9 | –95° | 27° | 43.2 | 112.39 |
| 1 | 10 | –95° | 32.30′ | 43.23 | 122.36 |
| 1 | 11 | –95° | 38° | 43.36 | 132.34 |
| 2 | 1 | –91°30′ | –16° | 52.29 | 32.48 |
| 2 | 2 | –91°30′ | –10°30′ | 51.79 | 42.05 |
| 2 | 3 | –91°30′ | –5° | 52.5 | 52.03 |
| 2 | 4 | –91°30′ | 0 | 52.13 | 61.38 |
| 2 | 5 | –91°30′ | 5° | 52.88 | 70.77 |
| 2 | 6 | –91°30′ | 10°30′ | 52.47 | 81.22 |
| 2 | 7 | –91°30′ | 16° | 53.1 | 91.68 |
| 2 | 8 | –91°30′ | 21°30′ | 52.51 | 102.13 |
| 2 | 9 | –91°30′ | 27° | 52.81 | 112.53 |
| 2 | 10 | –91°30′ | 32.30′ | 51.74 | 122.75 |
| 2 | 11 | –91°30′ | 38° | 51.34 | 132.77 |
| 3 | 1 | –88° | –16° | 58.88 | 32.48 |
| 3 | 2 | –88° | –10°30′ | 59.74 | 42.03 |
| 3 | 3 | –88° | –5° | 60.42 | 51.86 |
| 3 | 4 | –88° | 0 | 60.82 | 61.13 |
| 3 | 5 | –88° | 5° | 61.03 | 70.6 |
| 3 | 6 | –88° | 10°30′ | 61.07 | 81.14 |
| 3 | 7 | –88° | 16° | 60.98 | 91.73 |
| 3 | 8 | –88° | 21°30′ | 60.78 | 102.3 |
| 3 | 9 | –88° | 27° | 60.53 | 112.76 |
| 3 | 10 | –88° | 32.30′ | 60.29 | 122.03 |
| 3 | 11 | –88° | 38° | 60.14 | 133 |
| 4 | 1 | –84° | –16° | 68.65 | 33.42 |
| 4 | 2 | –84° | –10°30′ | 69.28 | 42.47 |
| 4 | 3 | –84° | –5° | 69.9 | 52.13 |
| 4 | 4 | –84° | 0 | 70.34 | 61.3 |
| 4 | 5 | –84° | 5° | 70.63 | 70.72 |
| 4 | 6 | –84° | 10°30′ | 70.77 | 81.26 |
| 4 | 7 | –84° | 16° | 70.73 | 91.89 |
| 4 | 8 | –84° | 21°30′ | 70.55 | 102.48 |
| 4 | 9 | –84° | 27° | 70.29 | 112.96 |
| 4 | 10 | –84° | 32.30′ | 70.01 | 123.2 |
| 4 | 11 | –84° | 38° | 69.81 | 133.11 |
| 5 | 1 | –80° | –16° | 78.8 | 34,06 |
| 5 | 2 | –80° | –10°30′ | 79.15 | 43.03 |
| 5 | 3 | –80° | –5° | 79.61 | 52.56 |
| 5 | 4 | –80° | 0 | 80.01 | 61.64 |
| 5 | 5 | –80° | 5° | 80.3 | 70.98 |
| 5 | 6 | –80° | 10°30′ | 80.46 | 81.47 |
| 5 | 7 | –80° | 16° | 80.45 | 92.06 |
| 5 | 8 | –80° | 21°30′ | 80.31 | 102.62 |
| 5 | 9 | –80° | 27° | 80.07 | 113.04 |
| 5 | 10 | –80° | 32.30′ | 79.8 | 123.21 |
| 5 | 11 | –80° | 38° | 79.61 | 133.01 |
| 6 | 1 | –76° | –16° | 89.16 | 34.7 |
| 6 | 2 | –76° | –10°30′ | 89.24 | 43.75 |
| 6 | 3 | –76° | –5° | 89.52 | 53.24 |
| 6 | 4 | –76° | 0 | 89.82 | 62.21 |

Continuation of Table 1

| 1 | 2 | 3 | 4 | 5 | 6 |
|---|---|---|---|---|---|
| 6 | 5 | –76° | 5° | 90.07 | 71.43 |
| 6 | 6 | –76° | 10°30′ | 90.22 | 81.77 |
| 6 | 7 | –76° | 16° | 09.24 | 92.19 |
| 6 | 8 | –76° | 21°30′ | 90.12 | 102.59 |
| 6 | 9 | –76° | 27° | 89.92 | 112.82 |
| 6 | 10 | –76° | 32.30′ | 89.7 | 122.75 |
| 6 | 11 | –76° | 38° | 89.57 | 133.25 |
| 7 | 1 | –72° | –16° | 99.59 | 34.7 |
| 7 | 2 | –72° | –10°30′ | 99.44 | 43.75 |
| 7 | 3 | –72° | –5° | 99.55 | 53.24 |
| 7 | 4 | –72° | 0 | 99.75 | 62.21 |
| 7 | 5 | –72° | 5° | 99.94 | 71.43 |
| 7 | 6 | –72° | 10°30′ | 100.08 | 81.77 |
| 7 | 7 | –72° | 16° | 100.1 | 92.19 |
| 7 | 8 | –72° | 21°30′ | 100.03 | 102.59 |
| 7 | 9 | –72° | 27° | 99.88 | 112.82 |
| 7 | 10 | –72° | 32.30′ | 99.72 | 122.75 |
| 7 | 11 | –72° | 38° | 99.67 | 132.25 |
| 8 | 1 | –68° | –16° | 109.95 | 34.62 |
| 8 | 2 | –68° | –10°30′ | 109.64 | 43.79 |
| 8 | 3 | –68° | –5° | 109.62 | 53.33 |
| 8 | 4 | –68° | 0 | 109.73 | 62.3 |
| 8 | 5 | –68° | 5° | 109.87 | 71.49 |
| 8 | 6 | –68° | 10°30′ | 109.99 | 81.76 |
| 8 | 7 | –68° | 16° | 110.04 | 92.11 |
| 8 | 8 | –68° | 21°30′ | 110.01 | 102.41 |
| 8 | 9 | –68° | 27° | 109.92 | 112.53 |
| 8 | 10 | –68° | 32.30′ | 109.85 | 122.34 |
| 8 | 11 | –68° | 38° | 109.89 | 131.69 |
| 9 | 1 | –64° | –16° | 120.13 | 34.32 |
| 9 | 2 | –64° | –10°30′ | 119.73 | 43.63 |
| 9 | 3 | –64° | –5° | 119.63 | 53.25 |
| 9 | 4 | –64° | 0 | 119.69 | 62.24 |
| 9 | 5 | –64° | 5° | 119.81 | 71.42 |
| 9 | 6 | –64° | 10°30′ | 120.02 | 81.66 |
| 9 | 7 | –64° | 16° | 120.01 | 91.95 |
| 9 | 8 | –64° | 21°30′ | 120.02 | 102.17 |
| 9 | 9 | –64° | 27° | 120.01 | 112.2 |
| 9 | 10 | –64° | 32.30′ | 120.01 | 121.91 |
| 9 | 11 | –64° | 38° | 120.13 | 131.18 |
| 10 | 1 | –60° | –16° | 130.02 | 33.88 |
| 10 | 2 | –60° | –10°30′ | 129.6 | 43.33 |
| 10 | 3 | –60° | –5° | 129.49 | 53.05 |
| 10 | 4 | –60° | 0 | 129.54 | 62.09 |
| 10 | 5 | –60° | 5° | 129.66 | 71.29 |
| 10 | 6 | –60° | 10°30′ | 129.81 | 81.52 |
| 10 | 7 | –60° | 16° | 129.93 | 91.78 |
| 10 | 8 | –60° | 21°30′ | 130 | 101.97 |
| 10 | 9 | –60° | 27° | 130.05 | 111.97 |
| 10 | 10 | –60° | 32.30′ | 130.1 | 121.7 |
| 10 | 11 | –60° | 38° | 130.18 | 131.08 |
| 11 | 1 | –56° | –16° | 139.52 | 33.39 |
| 11 | 2 | –56° | –10°30′ | 139.15 | 42.99 |
| 11 | 3 | –56° | –5° | 139.08 | 52.8 |
| 11 | 4 | –56° | 0 | 139.17 | 61.94 |
| 11 | 5 | –56° | 5° | 139.33 | 71.14 |
| 11 | 6 | –56° | 10°30′ | 139.53 | 81.46 |
| 11 | 7 | –56° | 16° | 139.7 | 91.76 |
| 11 | 8 | –56° | 21°30′ | 139.82 | 102.01 |
| 11 | 9 | –56° | 27° | 139.88 | 112.15 |
| 11 | 10 | –56° | 32.30′ | 139.84 | 122.18 |
| 11 | 11 | –56° | 38° | 139.54 | 130.02 |

Table 2

The input point's *P* coordinates and output angles $\varphi_{5i}$, $\varphi_{3j}$

| $i$ | $J$ | $\varphi_{5i}$ | $\varphi_{3_j}$ | $X_{P_{ij}}$ | $Y_{P_{ij}}$ |
|---|---|---|---|---|---|
| 1 | 2 | 3 | 4 | 5 | 6 |
| 1 | 1 | –95°11′ | –16°4′ | 43 | 33 |
| 1 | 2 | –95°28′ | –10°38′ | 43 | 43 |
| 1 | 3 | –95°29′ | –5°12′ | 43 | 53 |
| 1 | 4 | –95°23′ | 0°16′ | 43 | 63 |
| 1 | 5 | –95°17′ | 5°46′ | 43 | 73 |
| 1 | 6 | –9511′° | 11°14′ | 43 | 83 |
| 1 | 7 | –95°8′ | 16°39′ | 43 | 93 |
| 1 | 8 | –95°5′ | 22°3′ | 43 | 103 |
| 1 | 9 | –95°5′ | 27°26′ | 43 | 113 |
| 1 | 10 | –95°6′ | 32°51′ | 43 | 123 |
| 1 | 11 | –95°10 | 38°23′ | 43 | 133 |
| 2 | 1 | –90°34′ | –15°42′ | 53 | 33 |
| 2 | 2 | –90°58′ | –9°57′ | 53 | 43 |
| 2 | 3 | –91°12′ | –4°28′ | 53 | 53 |
| 2 | 4 | –91°18′ | 0°53′ | 53 | 63 |
| 2 | 5 | –91°19′ | 6°11′ | 53 | 73 |
| 2 | 6 | –91°17′ | 11°27′ | 53 | 83 |
| 2 | 7 | –91°13′ | 16°42′ | 53 | 93 |
| 2 | 8 | –91°9′ | 21°57′ | 53 | 103 |
| 2 | 9 | –91°4′ | 27°14′ | 53 | 113 |
| 2 | 10 | –91° | 32°36′ | 53 | 123 |
| 2 | 11 | –90°59′ | 38°7′ | 53 | 133 |
| 3 | 1 | –86°17′ | –16°1′ | 63 | 33 |
| 3 | 2 | –86°39′ | –10° | 63 | 43 |
| 3 | 3 | –86°56′ | –4°24′ | 63 | 53 |
| 3 | 4 | –87°6′ | 0°59′ | 63 | 63 |
| 3 | 5 | –87°11′ | 6°15′ | 63 | 73 |
| 3 | 6 | –87°12′ | 11°28′ | 63 | 83 |
| 3 | 7 | –87°10′ | 16°39′ | 63 | 93 |
| 3 | 8 | –87°5′ | 21°51′ | 63 | 103 |
| 3 | 9 | –86°49′ | 27°6′ | 63 | 113 |
| 3 | 10 | –86°53′ | 32°27′ | 63 | 123 |
| 3 | 11 | –86°17′ | 37°58′ | 63 | 133 |
| 4 | 1 | –82°15′ | –16°27′ | 73 | 33 |
| 4 | 2 | –82°29′ | –10°19′ | 73 | 43 |
| 4 | 3 | –82°44′ | –4°35′ | 73 | 53 |
| 4 | 4 | –82°55′ | 0°52′ | 73 | 63 |
| 4 | 5 | –83°2′ | 6°10′ | 73 | 73 |
| 4 | 6 | –83°5′ | 11°23′ | 73 | 83 |
| 4 | 7 | –83°4′ | 16°33′ | 73 | 93 |
| 4 | 8 | –82°59′ | 21°45′ | 73 | 103 |
| 4 | 9 | –82°53′ | 27° | 73 | 113 |
| 4 | 10 | –82°47′ | 32°23′ | 73 | 123 |
| 4 | 11 | –82°42′ | 37°57′ | 73 | 133 |
| 5 | 1 | –78°22′ | –16°49′ | 83 | 33 |
| 5 | 2 | –78°28′ | –10°38′ | 83 | 43 |
| 5 | 3 | –78°38′ | –4°50′ | 83 | 53 |
| 5 | 4 | –78°48′ | 0°41′ | 83 | 63 |
| 5 | 5 | –78°54′ | 6°2′ | 83 | 73 |
| 5 | 6 | –78°58′ | 11°16′ | 83 | 83 |
| 5 | 7 | –78°57′ | 16°28′ | 83 | 93 |
| 5 | 8 | –78°54′ | 21°41′ | 83 | 103 |
| 5 | 9 | –78°48′ | 26°59′ | 83 | 113 |
| 5 | 10 | –78°42′ | 32°24′ | 83 | 123 |
| 5 | 11 | –78°38′ | 38°3′ | 83 | 133 |
| 6 | 1 | –74°33′ | –17°1′ | 93 | 33 |
| 6 | 2 | –74°31′ | –10°52′ | 93 | 43 |
| 6 | 3 | –74°31′ | –5°3′ | 93 | 53 |

Continuation of Table 2

| 1 | 2 | 3 | 4 | 5 | 6 |
|---|---|---|---|---|---|
| 6 | 4 | –74°44′ | 0°31′ | 93 | 63 |
| 6 | 5 | –74°49′ | 5°54′ | 93 | 73 |
| 6 | 6 | –74°52′ | 11°11′ | 93 | 83 |
| 6 | 7 | –74°53′ | 16°26′ | 93 | 93 |
| 6 | 8 | –74°50′ | 21°41′ | 93 | 103 |
| 6 | 9 | –74°45′ | 27°1′ | 93 | 113 |
| 6 | 10 | –74°41′ | 32°31′ | 93 | 123 |
| 6 | 11 | –74°38′ | 38°15′ | 93 | 133 |
| 7 | 1 | –70°43′ | –17°4′ | 103 | 33 |
| 7 | 2 | –70°37′ | –10°58′ | 103 | 43 |
| 7 | 3 | –70°38′ | –5°10′ | 103 | 53 |
| 7 | 4 | –70°42′ | 0°25′ | 103 | 63 |
| 7 | 5 | –70°47′ | 5°50′ | 103 | 73 |
| 7 | 6 | –70°49′ | 11°9′ | 103 | 83 |
| 7 | 7 | –70°50′ | 16°26′ | 103 | 93 |
| 7 | 8 | –70°48′ | 21°45′ | 103 | 103 |
| 7 | 9 | –70°45′ | 27°9′ | 103 | 113 |
| 7 | 10 | –70°42′ | 32°43′ | 103 | 123 |
| 7 | 11 | –70°42′ | 38°33′ | 103 | 133 |
| 8 | 1 | –66°51′ | –16°57′ | 113 | 33 |
| 8 | 2 | –66°41′ | –10°57′ | 113 | 43 |
| 8 | 3 | –66°39′ | –5°11′ | 113 | 53 |
| 8 | 4 | –66°42′ | 0°23′ | 113 | 63 |
| 8 | 5 | –66°45′ | 5°49′ | 113 | 73 |
| 8 | 6 | –66°48′ | 11°10′ | 113 | 83 |
| 8 | 7 | –66°49′ | 16°30′ | 113 | 93 |
| 8 | 8 | –66°48′ | 21°51′ | 113 | 103 |
| 8 | 9 | –66°47′ | 27°19′ | 113 | 113 |
| 8 | 10 | –66°46′ | 32°58′ | 113 | 123 |
| 8 | 11 | –66°48′ | 38°54′ | 113 | 133 |
| 9 | 1 | –62°53′ | –16°43′ | 123 | 33 |
| 9 | 2 | –62°42′ | –10°49′ | 123 | 43 |
| 9 | 3 | –62°39′ | –5°6′ | 123 | 53 |
| 9 | 4 | –62°40′ | 0°26′ | 123 | 63 |
| 9 | 5 | –62°43′ | 5°52′ | 123 | 73 |
| 9 | 6 | –62°46′ | 11°14′ | 123 | 83 |
| 9 | 7 | –62°48′ | 16°36′ | 123 | 93 |
| 9 | 8 | –62°49′ | 21°59′ | 123 | 103 |
| 9 | 9 | –62°49′ | 27°30′ | 123 | 113 |
| 9 | 10 | –62°50′ | 33°11′ | 123 | 123 |
| 9 | 11 | –62°53′ | 39°10′ | 123 | 133 |
| 10 | 1 | –58°47′ | –16°26′ | 133 | 33 |
| 10 | 2 | –58°36′ | –10°37′ | 133 | 43 |
| 10 | 3 | –58°33′ | –4°59′ | 133 | 53 |
| 10 | 4 | –58°35′ | 0°32′ | 133 | 63 |
| 10 | 5 | –58°38′ | 5°25′ | 133 | 73 |
| 10 | 6 | –58°42′ | 10°47′ | 133 | 83 |
| 10 | 7 | –58°45′ | 16°9′ | 133 | 93 |
| 10 | 8 | –58°48′ | 21°33′ | 133 | 103 |
| 10 | 9 | –58°49′ | 27°3′ | 133 | 113 |
| 10 | 10 | –58°50′ | 32°42′ | 133 | 123 |
| 10 | 11 | –58°51′ | 38°30′ | 133 | 133 |
| 11 | 1 | –54°29′ | –16°39′ | 143 | 33 |
| 11 | 2 | –54°20′ | –10°57′ | 143 | 43 |
| 11 | 3 | –54°19′ | –5°23′ | 143 | 53 |
| 11 | 4 | –54°23′ | 0°32′ | 143 | 63 |
| 11 | 5 | –54°28′ | 5°27′ | 143 | 73 |
| 11 | 6 | –54°34′ | 10°46′ | 143 | 83 |
| 11 | 7 | –54°38′ | 16°6′ | 143 | 93 |
| 11 | 8 | –54°41′ | 21°26′ | 143 | 103 |
| 11 | 9 | –54°42′ | 26°48′ | 143 | 113 |
| 11 | 10 | –54°38′ | 32°8′ | 143 | 123 |
| 11 | 11 | –54°19′ | 37°4′ | 143 | 133 |

## 9. Discussion of the research results

The fulfilled studies show that three types of the output point's movements of the synthesized parallel manipulator in a cylindrical coordinate system, i. e. movements in two orthogonal directions and rotations around a vertical axis are carried out by separate drives. Therefore, in this case, there is a functionally independent operation of the drives, which leads to their kinematic and dynamic independents. In the existing methods for designing manipulating robots, control of the laws of motions of the drives is determined by solving the inverse kinematics problem with the simultaneous operation of all three drives. Therefore, an approach for the design of parallel manipulators proposed in this paper simplifies the control system and improves dynamic characteristics. However, at the same time, manipulators work with certain structural schemes and geometrical parameters of links, and this requires special methods of structural and parametric synthesis. The developed methods of structural-parametric synthesis allow dividing the problem of synthesis of parallel manipulators of complex structure into subproblems for the synthesis of their separate structural modules. The development of these methods in relation to spatial platform parallel manipulators is proposed.

## 10. Conclusions

1. Method of structural synthesis of a RoboMech class parallel manipulator with three DOF operating in a cylindrical coordinate system has been developed. This manipulator is formed by connecting the output point to the base using one passive and two active CKC.

2. Active CKC impose geometrical constraints on the movements of the output point, therefore they work at certain values of the geometrical parameters of their links. CKC synthesis parameters are determined on the base of Chebyshev and least-square approximations.

3. The direct and inverse kinematics problems of the synthesized manipulator are solved. Numerical results showed that the maximum deviation of the output point movement from the orthogonal trajectories is 1.65 %.

4. On the base of the numerical results analysis of the direct and inverse kinematics problems, it is found that there are functionally independent drives, i. e. orthogonal trajectories of the output point are reproduced by separate drives.

References


1. Baigunchekov, Z., Kalimoldayev, M., Ibrayev, S., Izmambetov, M., Baigunchekov, T., Naurushev, B., Aisa, N. (2016). Parallel Manipulator of a Class RoboMech. Mechanism and Machine Science, 547–557. doi: https://doi.org/10.1007/978-981-10-2875-5_45
2. Baigunchekov, Z., Ibrayev, S., Izmambetov, M., Baigunchekov, T., Naurushev, B., Mustafa, A. (2019). Synthesis of Cartesian Manipulator of a Class RoboMech. Mechanisms and Machine Science, 69–76. doi: https://doi.org/10.1007/978-3-030-00365-4_9
3. Baigunchekov, Z., Izmambetov, M., Zhumasheva, Z., Baigunchekov, T., Mustafa, A. (2019). Parallel manipulator of a class RoboMech for generation of horizontal trajectories family. Mechanisms and Machine Science, 1395–1402. doi: https://doi.org/10.1007/978-3-030-20131-9_137
4. Assur, L. V. (1913). Investigation of Plane Hinged Mechanisms with Lower Pairs from the Point of View of their Structure and Classification (in Russian): Part I. Bull. Petrograd Polytech. Inst., 20, 309–386.
5. Assur, L. V. (1914). Investigation of Plane Hinged Mechanisms with Lower Pairs from the Point of View of their Structure and Classification (in Russian): Part II. Bull. Petrograd Polytech. Inst., 21, 187–283.
6. Yang, T.-L., Sun, D.-J. (2012). A General Degree of Freedom Formula for Parallel Mechanisms and Multiloop Spatial Mechanisms. Journal of Mechanisms and Robotics, 4 (1). doi: https://doi.org/10.1115/1.4005526
7. Kutzbach, K. (1933). Einzelfragen aus dem Gebiet der Maschinenteile. Zeitschrift der Verein Deutscher Ingenieur, 77, 1168–1169.
8. Meng, X., Gao, F., Wu, S., Ge, Q. J. (2014). Type synthesis of parallel robotic mechanisms: Framework and brief review. Mechanism and Machine Theory, 78, 177–186. doi: https://doi.org/10.1016/j.mechmachtheory.2014.03.008
9. Burmester, L. (1988). Lehrbuch der Kinematik. Leipzig.
10. Schoenflies, A. (1886). Geometric der Bewegung in Synthetischer Darstellung. Leipzig.
11. Bottema, O., Roth, B. (1979). Theoretical Kinematics. North-Holland Publishing Company, 558.
12. Chebyshev, P. L. (1879). Sur Les Parallélogrammes Composés de Trois Éléments Quelconques. Mémoires de l'Académie des Sciences de Saint-Pétersbourg, 36, Suppl. 3.
13. Levitskii, N. I. (1950). Design of Plane Mechanisms with Lower Pairs. Moscow-Leningrad, 182.
14. Sarkisyan, Y. L., Gupta, K. C., Roth, B. (1973). Kinematic Geometry Associated With the Least-Square Approximation of a Given Motion. Journal of Engineering for Industry, 95 (2), 503–510. doi: https://doi.org/10.1115/1.3438183
15. Sarkissyan, Y. L., Gupta, K. C., Roth, B. (1973). Spatial Least-Square Approximation of a Motion. IFFToM Int. Symposium on Linkages and Computer Design Methods. Vol. B. Bucharest, 512–521.
16. Sarkisyan, Y. L., Gupta, K. C., Roth, B. (1979). Chebychev Approximations of Finite Point Sets with Application to Planar Kinematic Synthesis. Journal of Mechanical Design, 101 (1), 32–40. doi: https://doi.org/10.1115/1.3454021
17. Sarkisyan, Y. L., Gupta, K. C., Roth, B. (1979). Chebychev Approximations of Spatial Point Sets Using Spheres and Planes. Journal of Mechanical Design, 101 (3), 499–503. doi: https://doi.org/10.1115/1.3454084
18. McCarthy, J. M., Bodduluri, R. M. (2000). Avoiding singular configurations in finite position synthesis of spherical 4R linkages. Mechanism and Machine Theory, 35 (3), 451–462. doi: https://doi.org/10.1016/s0094-114x(99)00005-1
19. Plecnik, M. M., Michael McCarthy, J. (2015). Computational Design of Stephenson II Six-Bar Function Generators for 11 Accuracy Points. Journal of Mechanisms and Robotics, 8 (1). doi: https://doi.org/10.1115/1.4031124
20. Plecnik, M. M., McCarthy, J. M. (2016). Design of Stephenson linkages that guide a point along a specified trajectory. Mechanism and Machine Theory, 96, 38–51. doi: https://doi.org/10.1016/j.mechmachtheory.2015.08.015
21. Plecnik, M. M., McCarthy, J. M. (2016). Kinematic synthesis of Stephenson III six-bar function generators. Mechanism and Machine Theory, 97, 112–126. doi: https://doi.org/10.1016/j.mechmachtheory.2015.10.004